JPE 9-2-2

Control Algorithms of Large Synchronous Machines for Starting Gas Turbosets

Seon-Hwan Hwang*, Jang-Mok Kim†, Ho-Seon Ryu** and Gi-Gab Yoon***

†*Department of Electrical Engineering, Pusan National University, Korea
**Instrument & Control Group, Power Generation Lab., KEPRI, Korea
***Advanced Distribution System Group, Distribution Power System Lab., KEPRI, Korea

ABSTRACT

The static frequency converter (SFC) systems are used as a method of driving large synchronous machines in many power and industrial plants. In this paper, new control algorithms of SFC systems for starting gas turbosets are proposed for a four quadrant operation: start-up at standstill; an acceleration up to the speed of the rated voltage; field weakening to reach the rated speed; synchronization to the main alternating current (AC) source; and dynamic braking to stop safely within the rating of the synchronous machine. Experimental results show that the proposed algorithms are proper and effective.

Keywords: Static frequency converter, Large synchronous machine, Gas turbosets, Four quadrant operation

1. Introduction

A variety of systems has been developed over the years for starting synchronous machines and gas turbines; with the choice of method employed depending on the particular requirements and conditions in the supply network. With gas turbines, for instance, a rotating exciter or separate direct current (DC) motor has been used. As a result, there are many mechanical problems because the group of the machine is longer. A general system has been developed, the static starting device, which is adaptable to any specific requirements. In addition, the static starting device is not only capable of starting a synchronous motor up to a rated speed, but also of braking the motor from the rated speed to a standstill. The switching devices of a static frequency converter (SFC) are thyristors rather than insulated gate bipolar transistors (IGBTs). Thyristors are more reliable than IGBTs when subjected to overvoltage and overcurrent in a large scale power system. A synchronous machine is started from a standstill by applying a phase-synchronized variable frequency generated by a load commutated inverter (LCI) system. The starting system can be located remotely from the motor. In addition, one startup system can be applied to several motors [1]-[6]. This system can operate at all four

Manuscript received Nov. 14, 2008; revised Jan. 7, 2009
†Corresponding Author: jmok@pusan.ac.kr.
Tel: +82-51-510-2366, Fax: +82-51-513-0212, Pusan Nat'l Univ
*Department of Electrical Eng., Pusan National Univ., Korea
**Instrument & Control Group, KEPRI, Korea
***Advanced Distribution System Group, KEPRI, Korea

quadrants, so it can be used for driving, braking, or reversing large synchronous machines [3], [5]. In the electrical field, SFC systems are used for starting the synchronous motor/generators of gas turbines and pumped storage plants. These two machines have the same conceptual algorithms except for field weakening in the gas turbine. A gas turbine must be run up to about 60% of its rated speed before it is capable of producing enough power to continuously accelerate[2-3], [5]. Moreover, the rotating exciter or separate DC motor is located on the same shaft of the synchronous machine, and is used for the synchronous machine of the gas turbine. However, the SFC system has become the preferred method to start a large synchronous machine because it is easily adaptable to any specific requirements. Previous studies concentrated on the pulse (or forced) and the natural commutation at the first quadrant operation [3-5].

In this paper, control algorithms for an LCI system are proposed for starting a gas turbine in the four quadrants including start-up at standstill; acceleration up to the speed of the rated voltage and field weakening; and synchronization and dynamic braking to stop the machine safely within the machine rating of the synchronous machine. In particular, a proposed field-weakening algorithm is described with a detailed analysis of the synchronous machine in the field weakening region. Experimental results show that the proposed control algorithms are appropriate and effective for starting gas turbosets.

2. LCI System

Fig. 1 shows a schematic diagram of a load commutated inverter with the synchronous machine used to start gas turbines. The LCI system consists of a network converter (NC) and a machine converter (MC) producing the DC voltages V_{dc-con} and V_{dc-inv}, and DC link reactor L_{dc}, as shown in Fig. 1. The DC link decouples the different three-phase bridge frequencies and smoothes the rectified current I_{dc}.

In Fig. 1, the NC on the input side is connected to the main supply system and acts as a controlled rectifier during normal operation (i.e., the motoring operation). The MC on the machine side operates as an inverter. The output currents of the MC contain the fundamental and harmonic components simultaneously because the gating of the thyristor establishes the 120° conduction pattern.

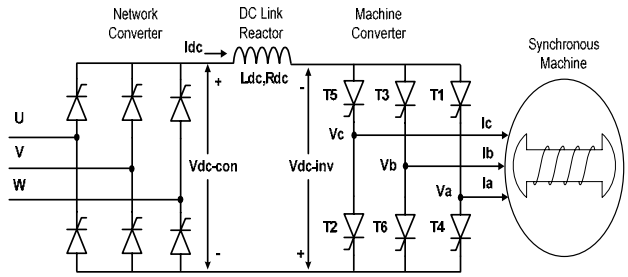

Fig. 1 Schematic of a load commutated inverter

Table 1 Relation of switching sequences and output currents

Mode	Mode 1	Mode 2	Mode 3	Mode 4	Mode 5	Mode 6
Current	T6,T1	T1,T2	T2,T3	T4,T5	T5,T6	T6,T1
Ia	Idc	Idc	0	-Idc	-Idc	0
Ib	-Idc	0	Idc	Idc	0	-Idc
Ic	0	-Idc	-Idc	0	Idc	Idc

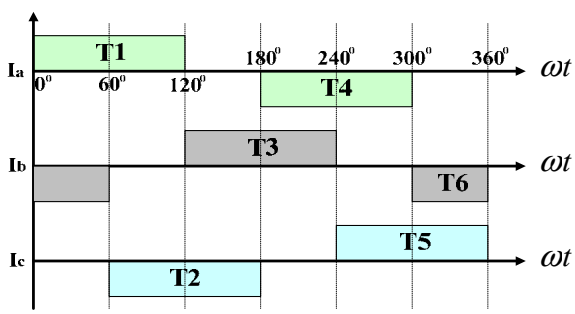

Fig. 2 Idealized output current waveforms of the machine converter

Another operation mode conducts during 60° of a period of the stator voltage of the synchronous machine.

Table 1 presents the relations of the switching sequences and the output currents. In Table 1, T1-T6 represent each thyristor in Fig. 1.

The output current waveforms of each phase are shown in Fig. 2. In Fig. 2, only two thyristors are simultaneously turned on during 60°, and the conduction angle of each phase is 120°.

3. Operating Modes

Fig. 3 shows the driving characteristic curves of the synchronous machine fed by the LCI system.

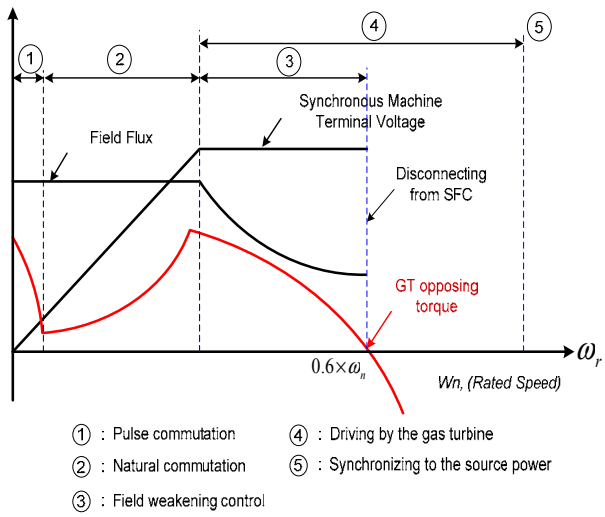

Fig. 3 Characteristics of load, terminal voltage, and field fluxlevel of the gas turbine

The operating ranges of the LCI system can be divided into driving, field weakening, synchronization, and braking modes. Driving mode consists of pulse (or forced) and natural commutation operations at the constant field flux region as shown in Fig. 3 [2-3], [5]. A field weakening operation is needed under the limited voltage condition to accelerate the motor with maximum torque, as shown in Fig. 3 ③. The synchronization operation occurs with an AC power system after the motor reaches the rated or synchronous speed to be run by the main AC power. The braking operation is necessary to stop the synchronous machine safely without mechanical stress on the shaft bearing.

3.1 Driving mode

In the driving mode, the NC on the input side functions as a rectifier, and the MC on the machine side operates as an inverter [1], [3], [5]. At a standstill, the amplitude of the machine voltage is zero, and commutation of the current in the MC can no longer be ensured by the machine voltage. Instead, at a very low speed, this is achieved by a pulse operation. Then, commutation is regulated by the NC rather than the motor voltage, as shown in Fig. 3 ①. Therefore, during the pulse operation or the left part of the driving range, a pulse operation or a forced commutation is needed by the NC [2], [5]. The firing angle γ of the MC is always controlled as described in Table I. As the motor speed is increased, the rate of change of the switching sequence is directly proportional to the motor speed. Fig. 4 shows a control block diagram of the driving mode of the LCI system with the synchronous machine.

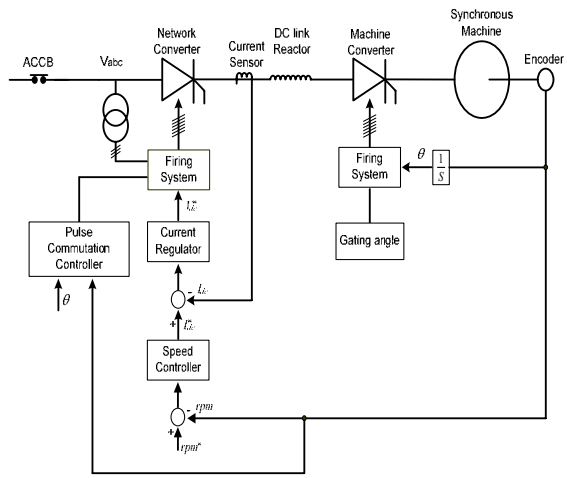

Fig. 4 Control block diagram of driving mode of LCI system with synchronous machine

In Fig. 4, the current and voltage references are developed by the speed controller and the current regulator in which the PI controller is adopted, respectively. As shown in Fig. 4, the firing system of the NC needs the phase angle of the AC power system for proper natural commutation, and the rotor position for pulse commutation at the low speed range. The MC only requires information of the rotor position for natural commutation. This control scheme is similar to general motor control [7-8].

3.2 Field weakening mode

To understand the coupling between the load commutated inverter and the synchronous machine, it is first necessary to examine the operation of the synchronous machine [6]. The synchronous machine will be analyzed using the *dq*-axes representation with

electrical angular velocity ω_e. The motor parameters are functions of the rotor position unless the *dq*-axes reference frame is assumed to be rotated synchronously with the motor.

The voltage equation of the cylindrical synchronous machine at the steady state can be written as

$$\begin{bmatrix} V_{ds}^r \\ V_{qs}^r \end{bmatrix} = \begin{bmatrix} R_s & -\omega_e L_s \\ \omega_e L_s & R_s \end{bmatrix} \begin{bmatrix} i_{ds}^r \\ i_{qs}^r \end{bmatrix} + \begin{bmatrix} 0 \\ \omega_e L_m i_{fd}' \end{bmatrix} \quad (1)$$

where V_{ds}^r and V_{qs}^r are *d*- and *q*-axis components of the stator terminal voltage, respectively, and i_{ds}^r and i_{qs}^r are *d*- and *q*-axis currents of the stator, respectively. L_s is the stator self-inductance, and R_s is the stator resistance.

The electromagnetic torque T_e is given by

$$T_e = \frac{3}{2} P \left[L_m i_{fd}' i_{qs}^r \right] \quad (2)$$

where P is the number of pole pairs, and $L_m i_{fd}'$ is the rotor flux linkage made by the rotor excitation system.

This equation does not suggest the vector control of the synchronous machine. In (1) and (2), these equations are introduced to help in understanding the field weakening operation described in this paper.

a) Operating limit conditions

The maximum available voltage $V_{s\,max}$ that the NC can supply to the machine is limited by the output voltage of the NC, as shown in (3)-(5):

$$V_{con-\max} = \frac{3\sqrt{2}}{\pi} V_{s-ll} \cos\alpha \quad (3)$$

where $V_{con\text{-}max}$ is the maximum output voltage of the NC, $V_{s\text{-}ll}$ is the line-to-line voltage of the AC source, and α is the firing angle of the NC.

From Fig. 1, the available output voltage of the machine converter can be expressed by

$$V_{inv-\max} = V_{inv-\max} - R_{dc} I_{dc-rate} \quad (4)$$

where $V_{inv\text{-}max}$ is the maximum output voltage of the MC, R_{dc} is resistance of the DC link, and $I_{dc\text{-}rate}$ is the rated current. As a result, the maximum output voltage of the MC, $V_{s\max}$, is

$$V_{s\max} = \left| V_{inv-\max} \frac{\pi}{3\sqrt{3}\cos\gamma} \right| = \left| \left(\frac{3\sqrt{2}}{\pi} V_{s-ll} - R_{dc} I_{dc-rate} \right) \frac{\pi}{3\sqrt{3}\cos\gamma} \right| \quad (5)$$

In (5), V_{smax} is proportional to the amplitude of the line-to-line voltage of the AC source, and to the firing angle of the NC. However, the firing angle of MC, γ, has the full firing angle of zero for natural commutation. The maximum current $I_{s\max}$ of the synchronous machine is limited by the MC's current rating and machine thermal rating. Therefore, the voltage and current limit conditions of the synchronous machine for the operation of the field weakening region are defined as [9]-[11]:

$$V_{ds}^{r\,2} + V_{qs}^{r\,2} \le V_{s\max}^{\ 2} \quad (6)$$

$$i_{ds}^{r\ 2} + i_{qs}^{r\ 2} \le I_{s\max}^{\ 2} \quad (7)$$

b) Proposed field weakening algorithm

In order to drive the synchronous machine for starting the gas turbine effectively in the field weakening region, two factors must be considered. One is the optimal starting speed of the field weakening, and the other is the optimal current trajectory to produce maximum torque. According to the load and machine conditions, including the excitation of the field winding, the saturation of the PI current regulator varies. Therefore, the starting speed of the field weakening must be changed. The early starting of the field weakening may cause a drop in output torque, even in the constant torque region. Late starting results in saturation of the current regulator such that the control performance of the starting system degrades. Accordingly, it is necessary to change the starting point of the field weakening operation according to load and machine conditions. From (1) and (6), the optimal starting speed can be derived as

$$\omega_b = \frac{V_{s\max}}{L_m\sqrt{\left(i_{ds}^r + i_{fd}{}'\right)^2 + \left(i_{qs}^r\right)^2}} \tag{8}$$

In (8), the optimal starting speed is varied according to the maximum available voltage, the stator current, the excitation current, and the load condition. However, it is difficult to derive the exact starting speed of field weakening without the precise machine parameters.

The voltage limit circle can be derived using (1) and (6)

$$\left(\frac{V_{s\max}}{\omega_r L_m}\right)^2 = \left(i_{ds}^r + i_{fd}{}'\right)^2 + \left(i_{qs}^r\right)^2 \tag{9}$$

The voltage drop due to resistance is ignored to simplify the resulting equation. Thus, the rotor excitation current can be obtained as

$$i_{fd}{}' = \sqrt{\left(\frac{V_{s\max}}{\omega_r L_m}\right)^2 - \left(i_{qs}^r\right)^2} - i_{ds}^r \tag{10}$$

Fig. 5 shows the current limit circle of the *dq*-axes synchronous reference frame. In Fig. 5, i_{ds}^r, i_{qs}^r are the *d*-and *q*-axis currents, respectively. The voltage limit circle is nearly constant according to the variation of the motor speed in the constant field operation region. This is because the terminal voltage is nearly proportional to the increase of the motor speed.

In (9), the radius of the voltage limit circle, $V_{s\max}/L_m\omega_r$, is decreased about the variation of the motor speed. The current limit circle $I_{s\ max}$ is always constant.

The control of the SFC for driving the synchronous machine is possible in both the voltage limit circle and the current limit circle, as shown in Fig. 5. The voltage limit circle decreases according to the motor speed so that the PI current regulator is saturated quickly due to the lack of a control voltage in the field-weakening region. Therefore, the total area of the produced torque is reduced.

Fig. 5(a) shows the operating characteristics of the synchronous machine without the field weakening operation at the constant torque region.

In this region, the produced torque is nearly constant because the margin of the voltage is enough to accelerate the synchronous machine.

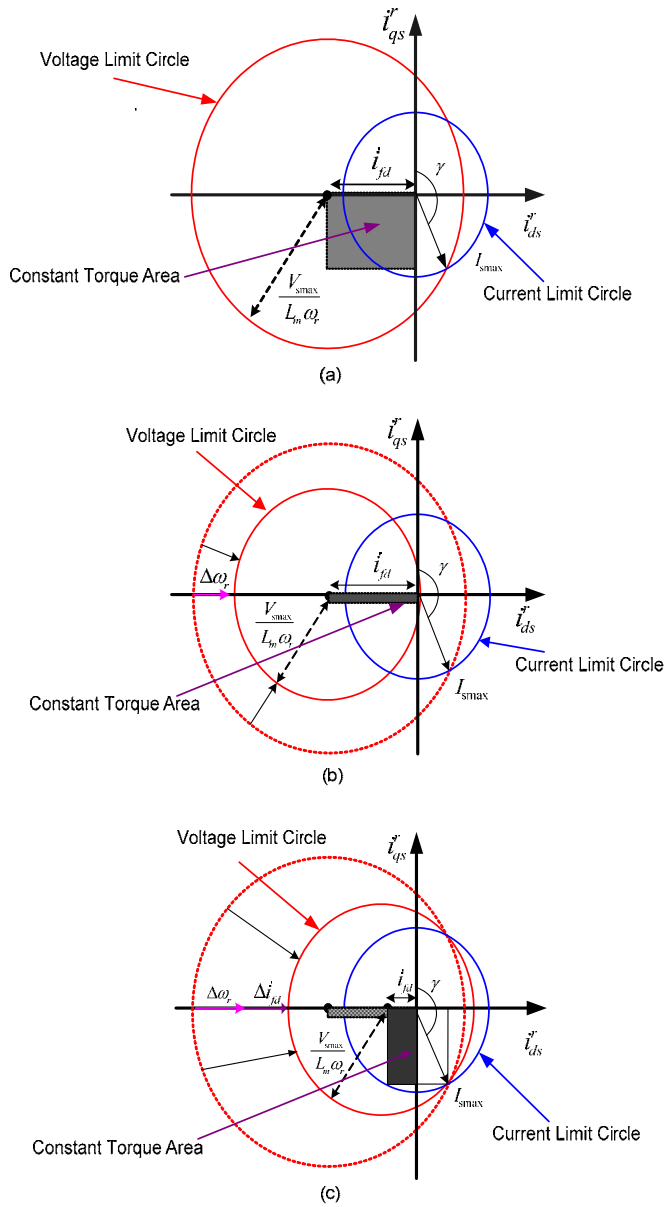

Fig. 5 Voltage and current limit diagram for maximum torque operation: (a) Operation of the constant torque region (b) Operation of constant field current control (c) Operation of the field weakening control

Fig. 5(b) shows the operating characteristics of the synchronous machine with constant field current control in the field weakening region. In this case, the center of the

voltage limit stays at the fixed point ($-i_{fd}'$, 0), so the operating area is reduced to rapidly regulate the stator current.

Fig. 5(c) shows the operating characteristics of the synchronous machine with field weakening control in the field-weakening region. The voltage limit circle decreases according to the motor speed, but the rotor field excitation also decreases so that the center of the voltage limit circle moves to the left of the *d*-axis as shown in Fig. 5(c). The total area of control is slightly reduced, but the voltage margin is enough to regulate the stator current in the high speed region. The produced torque is larger than without the field weakening control in this field weakening region. Therefore, the synchronous machine can be rapidly accelerated within the voltage and current ratings. However, it is not easy to obtain optimal current trajectory of the *dq*-axes synchronous reference.

Fig. 6 shows a block diagram of the proposed field weakening control for the gas turbine. At low and intermediate speeds, the magnitude of voltage command vector V_{dc}^{*}, which is the output of the PI current regulator of the NC to regulate the DC link current, is less than $V_{s\,max}$. There is no feed signal at the feedback loop of the anti-windup controller, as shown in Fig. 6.

In this case, the field weakening algorithm is not activated. As the operating frequency increases, V_{dc}^{*} finally reaches $V_{s\,max}$. The field weakening operation must then begin above this speed because there is a feedback signal at the anti-windup controller. As is known from the proposed field weakening algorithm, the field weakening operation is automatically achieved by using the feedback signal of the anti-windup without any information about machine speed, load conditions, and machine parameters,

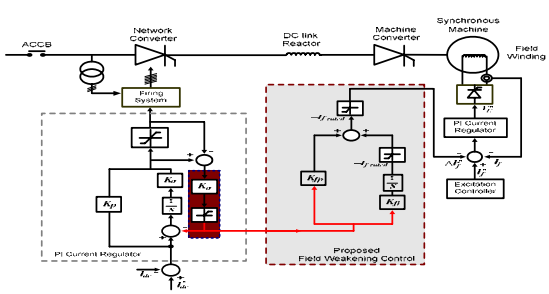

Fig. 6 Overall block diagram of the proposed field weakening algorithm

except for the feedback signal of the anti-windup controller. Therefore, the proposed field weakening algorithm has the attractive features of easy implementation, and robustness to variation in machine parameters and load conditions

3.3 Synchronization

Fig. 7 shows the control block diagram of the synchronization. Generally, the synchronous machine for starting the gas turbine must be brought up to 60% of its rated speed, and is then operated by the gas turbine. The turbine accelerates the machine up to rated speed to synchronize it with the AC network. To achieve synchronization, the phase angle of the AC power supply and the terminal voltage of the synchronous machine are detected and compared. When both sides of the phase angle are nearly the same and one of the phase voltages passes through zero crossing, then the line connection will be smoothly completed. Firstly, SW1 and SW 2 are off, and then SW3 is on to connect the machine to the AC power supply.

3.4 Braking mode

The braking operation is needed to obtain electric energy from the kinetic potential of the motor moving groups, and to smoothly stop the synchronous machine within the current rating when it is disconnected from a main AC source. Without the regeneration braking method, some of the kinetic energy generated by the moving groups may be dissipated as heat is lost in the distributed stator winding or the shaft bearing. However, the rest of the energy will be transferred through the DC link to the AC source if the proper control method of regeneration braking is adopted. During the braking operation, the back EMF of the motor functions as an AC source, the output voltage of the DC link is negative, and the DC link current is nearly constant. The MC functions not as an inverter, but as a rectifier, which regulates the constant extinction angle γ according to the rotor position for proper commutation and transfers the kinetic energy from the moving groups of the motor to the main AC source. The NC tries to transfer the maximum kinetic energy from the moving groups to the main AC source, but the rated

current of the synchronous machine is limited. Therefore, the NC transfers the maximum available energy to the main AC source within the current rating to safely and smoothly stop the machine without mechanical stress on the shaft bearing. A control block diagram of the regeneration braking is the same as shown in Fig. 4.

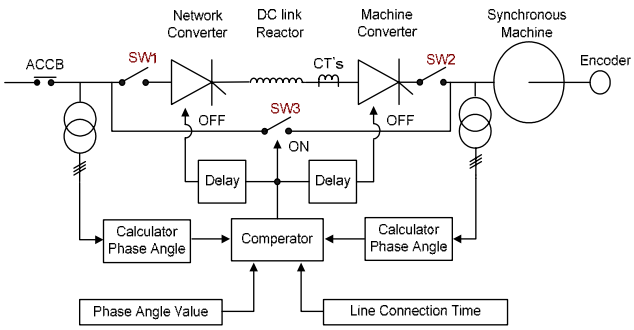

Fig. 7 Control block diagram of the line connection for synchronization with AC power

groups may be dissipated as heat losses in the distributed stator winding or the shaft bearing. However, the rest of the energy will be transferred through the dc link to the ac source if the proper control method of regeneration braking is adopted. During the braking operation, the back EMF of the motor functions as an ac source, the output voltage of the dc link is negative, and the dc link current is nearly constant. The MC functions not as an inverter but a rectifier, regulates the constant extinction angle γ according to the rotor position for proper commutation, and transfers the kinetic energy from the moving groups of the motor to the main ac source. The NC tries to transfer the maximum kinetic energy from the moving groups to the main ac source, but the rated current of the synchronous machine is limited. Therefore, the NC transfers the maximum available energy to the main ac source within the current rating to stop the machine safely and smoothly without mechanical stress on the shaft bearing. A control block diagram of the regeneration braking is the same as shown in Fig. 4.

4. Experimental Results

The parameters of the synchronous machine are shown in the Appendix. The drive system for the experiments was implemented with two TMS320VC33 DSP control boards as shown in Fig. 8. One board was used to control the NC and MC. The other was used to control the excitation system of the field winding of the synchronous machine. The firing of all thyristors was implemented on the NC, MC, and excitation system by using the field programmable gate array (FPGA) of the DSP control board.

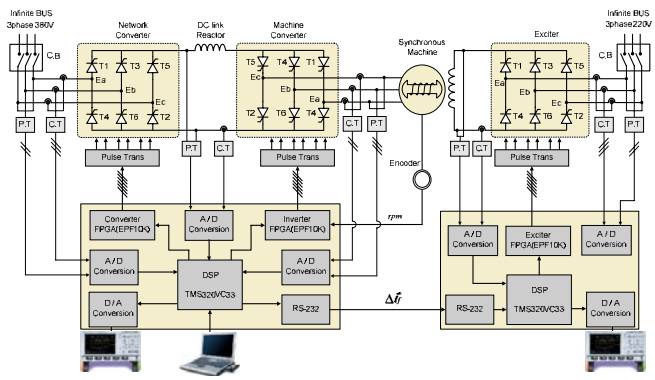

Fig. 8 Overall drive block diagram of LCI-synchronous machine and the excitation system

4.1 Driving mode

Fig. 9 shows the experimental results of the driving mode. The speed waveform for starting the synchronous machine from 0 to 1800 rpm is shown in Fig. 9(a). Below 200 rpm, the amplitude of the stator voltage is too small to commutate the stator current. Thus, the pulse operation is employed to chop the DC link current for proper commutation at the MC as shown in Fig. 9(b). From this waveform, there is a difference between the pulse operation and the natural commutation operation. Fig. 9(c) shows the waveform of the DC link voltage. The amplitude of the DC link voltage is proportional to the motor speed. After the motor speed reaches 1800 rpm, the DC link voltage is nearly constant.

4.2 Field weakening mode

Figs. 10 and 11 show the same experimental conditions except for the field weakening operation. As known from Figs. 10(c) and (d), the DC link current does not remain constant at the high speed range because the current regulator is already saturated due to a lack of supply voltage. As shown in Fig. 11, the DC link current remains

constant during the acceleration because there is a considerable voltage margin to regulate the machine current, even in the field weakening region, due to the proposed field weakening algorithm. As a result, the motor speed increases as shown from Fig. 11(d). Therefore, the experimental results show the usefulness of the proposed field weakening algorithm.

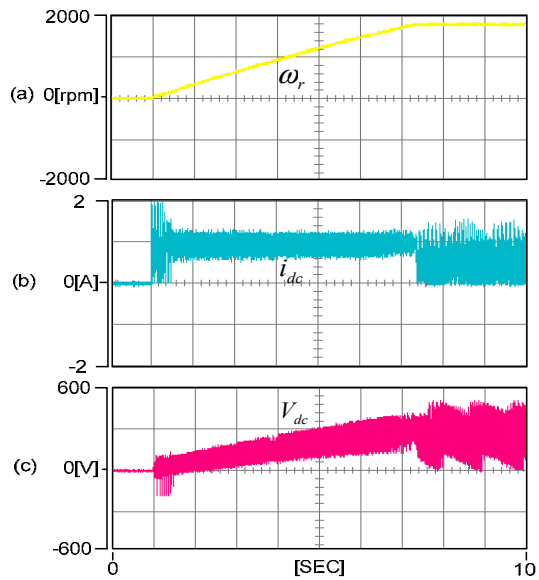

Fig. 9 Experimental results of the driving mode (a) Motor speed (b) DC link current (c) DC link voltage

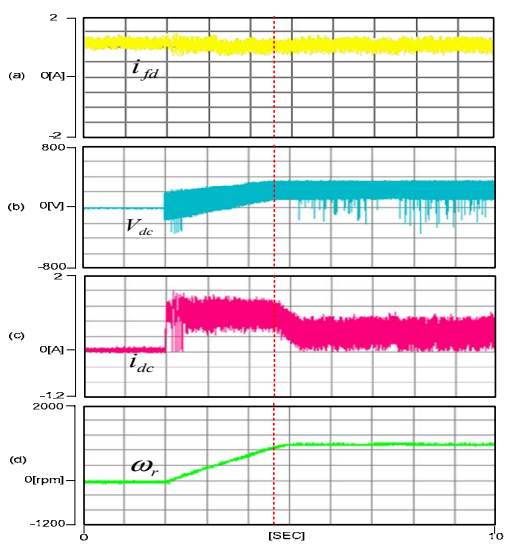

Fig. 10 Experimental results of the constant field control (a) Field current (b) DC link voltage (c) DC link current (d) Motor speed

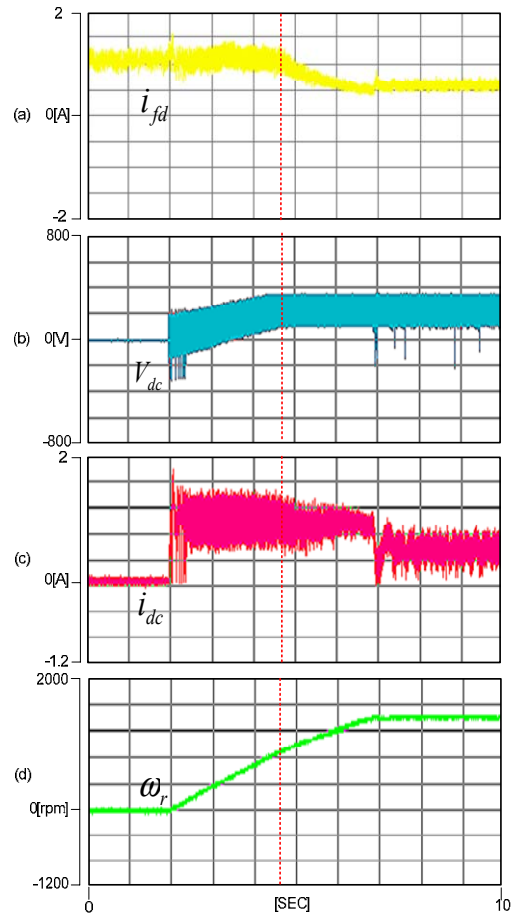

Fig. 11 Experimental results of the proposed field weakening algorithm (a) Field current (b) DC link voltage (c) DC link current (d) Motor speed

4.3 Synchronization mode

During synchronization, line connection is performed between the synchronous machine and the main AC power. Fig. 12 shows the experimental results of line connection. The beginning point of the synchronization is from the upward arrow (↑) in Fig. 12(a) and the downward arrow (↓) in Figs. 12(c) and (d). In Figs. 12(a) and (b), the experimental waveforms show the operation of the line connection when both phase angles of the NC and MC are the same, and one of these phase voltages passes through zero-crossing. As a result, the experimental waveforms of the motor voltage and the stator current show smooth synchronization operation and the usefulness of the proposed line connection algorithm in Figs. 12(c) and (d).

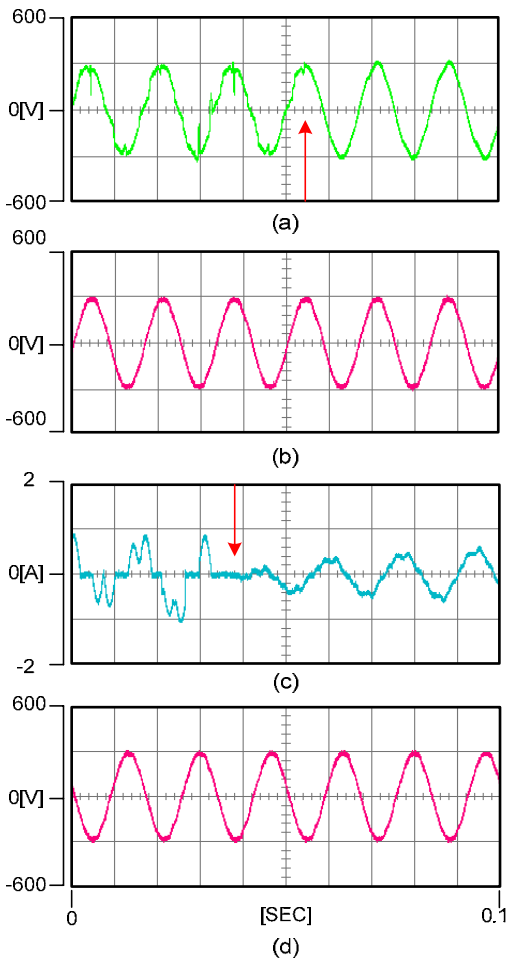

Fig. 12 Experimental results of synchronization with ac source: (a) Phase voltage of machine side (b) Phase voltage of source side (c) Phase current of machine side (d) Phase voltage of machine side

4.4 Braking mode

Fig. 13 shows the experimental waveforms in the braking mode operation. Fig. 13(a) shows the variation of the speed reference from 1,800 to 0 rpm for the dynamic braking mode operation. Fig. 13(b) shows the DC link current, which is regulated within the rated current. The characteristics of the motor speed, DC link current, and voltage show the usefulness of the proposed braking mode algorithm. Fig. 13(c) shows the variation of the DC link voltage from negative to zero, which demonstrates that the DC link current is constant, and the amplitude of the DC link voltage is reduced in proportion to the motor speed. From several experimental results, the proposed regenerative braking algorithm is practical and useful.

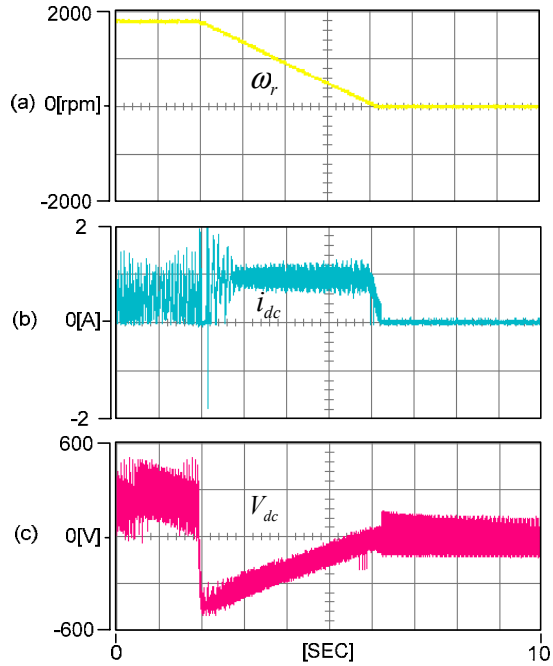

Fig. 13 Experimental results of the regeneration braking mode: (a) Motor speed (b) DC link current (c) DC link voltage

5. Conclusions

In this paper, the new control algorithms is proposed for a synchronous machine drive system using a load commutated inverter in four quadrant ranges including start-up from standstill, acceleration up to the rated speed, synchronization, and dynamic braking to save energy and safely and quickly stop the machine within the machine rating of the synchronous motor. For high speed operation, a new field weakening algorithm was proposed with a detailed analysis. The proposed field weakening method has no dependence on motor speed or machine parameters.

Experimental results show the validity of the proposed control algorithms for the operation of an LCI system to drive a gas turbine.

Appendix

Synchronous machine data:

Rated power = 900W, Rated voltage = 400V,

Rated current = 1A, Rated speed = 1800r/min, R = 8.5Ω,

Poles = 4, Field current = 1.15A, Xbase = 133.3Ω

Acknowledgment

This work is the outcome of a Manpower Development Program for Energy & Resources supported by the Ministry of Knowledge and Economy (MKE).

References

[1] David Finney, "Variable frequency AC motor drive systems", Peter PeregrinusLtd., pp.202-274, 1988.

[2] O. Kolb, F. Pender, and V. Suchanek, "Static starting equipment for gas turbosets", Brown Boveri Rev. 66, pp.104-112, 1979.

[3] F. Peneder, R. Lubasch, and A. Vonmard, "Static equipment for starting pumped storage plant, synchronous condensers and gas turbine sets", Brown Boveri Rev. 61, pp.440-447, 1974.

[4] R.S. Colby, M.D. Otto, and J.T. Boys, "Analysis of LCI synchronous motor drives with finite DC link inductance", *in Proc. IEE*, Vol.140, No.6, pp.379 -386, Nov., 1993.

[5] B. Mueller, T. Spinanger, and D. Wallstein, "Static variable frequency starting and drive system for large synchronous motors", *IEEE-IAS Conf.*, pp.429-438, Sept./Oct., 1979.

[6] ALLAN B. PLUNKETT, "System design method for a load commutated inverter-synchronous motor drive", *IEEE Trans. Ind. Appl.*, Vol.IA-20, No.3, May/June, 1984.

[7] P.C. sen, "Thyristor DC drives", John Wiley & Sons, N.Y., 1981.

[8] P. Kundur, "Power system stability and control", McGraw-Hill, Inc., pp.500-523, 2003.

[9] T.M. Jahns, "Flux-weakening regime operation of an interior permanent-magnet synchronous motor drive", *IEEE Trans. Ind. Appl.*, Vol.21, pp.681-689, July/Aug., 1987.

[10] B.K. Bose, "A high-performance inverter-fed drive system of an interior permanent-magnet synchronous machine", *IEEE Trans. Ind. Appl.*, Vol.24, pp.987-997, Nov./Dec., 1988.

[11] S. Morimoto, Y. Takeda, T. Hirasa, and K. Taniguchi, "Expansion of operating limits for permanent magnet motor by current vector control considering inverter capacity", *IEEE Trans. Ind. Appl.*, Vol.26, pp.866-871, Sep./Oct., 1990.

Seon-Hwan Hwang was born in Cheongyang, Korea, in 1978. He received the B.S. and M.S. degrees in Electrical Engineering from Pusan National University, Busan, Korea, in 2004 and 2006, respectively. He is currently working toward the Ph.D. at Pusan National University. His research interests are power conversion and electric machine drives.

Jang-Mok Kim was born in Busan, Korea, in August 1961. He received the B.S. degree from Pusan National University in 1988, and his M.S. and Ph.D. degrees from Seoul National University, Korea, in 1991 and 1996, respectively, in the department of Electrical Engineering. From 1997 to 2000, he was a senior research engineer with Korea Electrical Power research institute (KEPRI). Since 2001, he has been with the department of Electrical Engineering, Pusan National University (PNU), where he is currently a Faculty member. In addition, he is a research member of the research institute of Computer Information and Communication in PNU. His present interests are the control of the electric machines, electric vehicle propulsion, and power quality.

Ho-Seon Ryu was was born in Daejeon, Korea, in 1970. He received the B.S. and M.S. degrees in Electrical Engineering from Chung-Nam National University, Daejeon, Korea, in 1993 and 1995, respectively. He is working as a senior member in the Instrument & Control Group at KEPRI. His research interests are excitation system, high power inverter and static frequency converters, etc.

Gi-Gab Yoon received the B.S., M.S., and Ph. D. degrees in Electrical Engineering from Hanyang University, Seoul, Korea, in 1983, 1988, and 1999. He has over 15 years of research experience in the field of power systems. He is presently a senior researcher in Distribution power system laboratory and advanced distribution system group at KEPRI. His research field includes wind power generation system, distributed generation system, and control of power system.